Parasites & Vectors

RESEARCH Open Access

Climate and landscape features associated with successful *Wolbachia* replacement in the municipality of Rio de Janeiro, Brazil

Katie Tiley[1,2,3*], Katie Milligan Susong[1,2], Steffen Knoblauch[4,5], Kathleen M. O'Reilly[1,2] and Oliver J. Brady[1,2]

Abstract

Background *Wolbachia* replacement is a promising strategy for reducing arboviral transmission by *Aedes aegypti*. *Wolbachia* infection is refractory to arboviruses, including dengue and chikungunya, and *Wolbachia* spreads in mosquito populations by maternal transmission and cytoplasmic incompatibility, whereby mating between infected males and uninfected females produce nonviable offspring. Deployment programmes seek to establish stable, high *Wolbachia* prevalence through the release of *Wolbachia*-infected mosquitoes; however, prevalence varies spatially, particularly in complex urban environments where fine-scale heterogeneity in temperature and built environment may influence mosquito population dynamics. Here, we investigate how climate and landscape features are associated with heterogeneous *Wolbachia* replacement outcomes using *w*Mel prevalence data from releases in the municipality of Rio de Janeiro, Brazil (2017–2019).

Methods Across a 26-month period, 500 × 500 m spatial units were clustered into four distinct replacement trajectories: unsuccessful, low, moderate, and high success, defined using predicted *Wolbachia* prevalence time series generated from cell-level binomial regression models and grouped using k-means clustering. Associations were explored between each trajectory and features related to *Ae. aegypti* habitat suitability, climate sensitivity, flight barriers, and *Wolbachia* deployment barriers using a multinomial generalised additive model (GAM). We used forward selection based on Akaike Information Criterion, explicit consideration of spatial autocorrelation and screening for collinearity among covariates. Of the 23 covariates examined, four covariates were retained: proportion of tall buildings (% > 6 m in height), average air temperature (°C), average elevation (m above sea level), and average daily rainfall (mm).

Results Results show high replacement success was mostly associated with areas with fewer tall buildings [$\beta = -0.93$ (95% CI −1.43, −0.44), $P < 0.001$] and higher temperatures [$\beta = 1.11$ (95% CI 0.59, 1.62), $P < 0.001$], while higher elevation and lower rainfall were associated with poorer outcomes. These associations may also reflect unmeasured socioeconomic or infrastructure variation, and context-dependent temperature effects on mosquito and *Wolbachia* fitness. Model-based predictions indicate non-linear dynamics, with areas of more tall buildings and higher temperatures showing divergent predicted outcomes towards either high success or failure rather than intermediate replacement. Residual spatial clustering suggests additional neighbourhood-scale processes not captured by the available covariates.

*Correspondence:
Katie Tiley
katherine.tiley.21@ucl.ac.uk
Full list of author information is available at the end of the article

© The Author(s) 2026. **Open Access** This article is licensed under a Creative Commons Attribution 4.0 International License, which permits use, sharing, adaptation, distribution and reproduction in any medium or format, as long as you give appropriate credit to the original author(s) and the source, provide a link to the Creative Commons licence, and indicate if changes were made. The images or other third party material in this article are included in the article's Creative Commons licence, unless indicated otherwise in a credit line to the material. If material is not included in the article's Creative Commons licence and your intended use is not permitted by statutory regulation or exceeds the permitted use, you will need to obtain permission directly from the copyright holder. To view a copy of this licence, visit http://creativecommons.org/licenses/by/4.0/.

Conclusions Outcomes in high-rise and topographically complex areas appear less likely to stabilise at intermediate replacement. Such areas may require higher release densities, targeted supplemental interventions, and more intensive monitoring, although these remain as hypotheses requiring empirical evaluation. Through iterative modelling, it is possible to support rapid hypothesis identification to inform field tests and operational refinement as more evidence becomes available. These findings reinforce the role of urban permeability, vertical structure, and local environmental conditions in shaping the outcomes of *Wolbachia* replacement programmes.

Keywords *Wolbachia* replacement, *Aedes aegypti*, Modelling, Spatial heterogeneity, Rio de Janeiro

Background

Aedes aegypti are the primary vectors of dengue virus (DENV) across tropical and subtropical regions [1], where dengue imposes a substantial public health burden, with an estimated 96 million cases, 1.9 million DALYs and approximately 9,000 deaths annually [2]. The global distribution of *Ae. aegypti* is expanding [3], exacerbated by increased urbanisation [4] which increases availability of artificial breeding sites [5, 6].

While dengue vaccine development is promising [7–10], vector control remains a cornerstone of dengue control [2]. Conventional interventions include insecticides [11], larvicides [12], and limiting biting and reducing breeding habitats through community engagement and public works development [13, 14]. In recent decades, *Wolbachia* replacement has garnered interest as an intervention based on transinfection of *Ae. aegypti* with non-native *Wolbachia* strains (e.g. *w*Mel) which reduce dengue transmission in vector populations. *Wolbachia* are heritable intracellular bacteria which evolved as reproductive parasites in many arthropods [15], proliferating within populations through cytoplasmic incompatibility, whereby *Wolbachia*-infected males and uninfected females produce nonviable offspring [15–17]. Crucially, laboratory experiments demonstrate *Ae. aegypti* mosquitoes transinfected with *Wolbachia* exhibit refractoriness to dengue, Zika, and chikungunya viruses [18–22].

Experiments demonstrate that releasing *Wolbachia*-infected *Ae. aegypti* into uninfected populations results in successful replacement, i.e. population *Wolbachia* infection prevalence of > 90%, within a few generations [18, 23]. Theoretically, once *Wolbachia* infection prevalence crosses a critical population threshold, heritability and cytoplasmic incompatibility lead to continued proliferation without the need for additional intervention [17]. This threshold depends on strain characteristics, host fitness costs, maternal transmission efficiency, and local ecological conditions. Field releases have shown that *Wolbachia* replacement can achieve high, self-sustaining prevalence, but releases in some settings have also shown sustained intermediate prevalence (population infection prevalence < 60%), spatially heterogeneous ('patchy') replacement, or post-deployment loss of infection [20, 24, 26 –]. Imperfect *Wolbachia* replacement may still offer some benefits, intermediate replacement is reported to be associated with intermediate dengue transmission control in some settings [22]. Concerningly, deployments in the municipality of Rio de Janeiro found *Wolbachia* replacement is negatively correlated with dengue incidence [22], suggesting that areas with higher dengue transmission may present ecological or operational conditions less favourable to *Wolbachia* replacement. Understanding the factors associated with successful replacement could help identify opportunities to improve deployment effectiveness.

Wolbachia infection can impose context-dependent fitness costs on *Ae. aegypti*, including reduced egg viability, altered development, and reduced stress tolerance [27–35]. However, there are uncertainties on the influence of landscape features on *Wolbachia* infection dynamics. Spatial barriers which limit mosquito dispersal, such as highways [36, 37], and sudden changes in mosquito population densities [38] negatively impact *Wolbachia* spread. *Ae. aegypti* life history traits and breeding habitat availability are impacted by environmental factors such as temperature, humidity and rainfall [39, 40], vegetation cover [41, 42], and anthropological infrastructure [43–46]. Abrupt changes in climate, such as strong seasonal effects or extreme weather events, may also limit replacement [47–49]. For example, high temperatures from heatwaves may reduce bacterial density and lead to *Wolbachia* loss [50–52]. Researchers have speculated this is one reason for the unstable replacement reported after field deployments in Vietnam [25], however, the authors explicitly suggest undetermined elements of the built environment may affect *Wolbachia* replacement since replacement has been successful in other settings with analogous temperature profiles. In the case of Colombia [24, 53] and Brazil [20, 26], researchers suggest variable release intensity, due to logistical deployment limitations, and significant baseline variation in *Ae. aegypti* populations may have contributed to spatially heterogeneous replacement. Improving our understanding of landscape features on *Wolbachia*

infection dynamics is essential for realising the maximum efficacy of *Wolbachia* replacement in diverse settings.

Mathematical models have been used to explore how release strategy, mosquito dispersal, habitat quality and fitness costs influence *Wolbachia* establishment across heterogeneous environments [48, 54, 58 –]. Using publicly available data of deployments in the municipality of Rio de Janeiro, we develop a multinomial generalised additive model (GAM) which explores factors associated with *Wolbachia* infection prevalence trajectories to answer the research question: to what degree do climate and landscape features shape spatially heterogeneous *Wolbachia* replacement?

Methods

Releases in the municipality of Rio de Janeiro

After an initial pilot in 2014, described in Garcia et al. [59], 67 million *Wolbachia*-infected mosquitoes were released across an 86·8 km^2 area in the municipality of Rio de Janeiro in five stages (across three release zones) between August 29, 2017, and December 27, 2019. The pilot identified widespread insecticide resistance in baseline *Ae. aegypti* populations; thus, released mosquitoes were locally backcrossed with an insecticide-resistant *w*Mel strain. A network of BG-Sentinel traps ($n=1168$) was used to monitor *w*Mel prevalence in *Ae. aegypti* every 2 weeks over the release period.

This study uses public data provided by Ribeiro dos Santos et al. [22], available at https://github.com/pdg-cam/wMel_Rio_dengue_chik, accessed March 5, 2025. The data include the number of traps/collections, *Ae. aegypti* captured, mosquitoes tested positive for *w*Mel, and proportion *w*Mel. The data are spatially aggregated to a grid of raster cells ($n=396$), each 500×500 m, with an irregular boundary and temporally aggregated monthly from August 2017 until September 2019 inclusive. Although releases continued until December 2017, the publicly available dataset covers the period up to September 2019 and therefore all analyses are restricted to this timeframe. See data source [22] for complete details of data collection.

Outcome: wMel replacement trajectories

For each raster cell, monthly *w*Mel prevalence was calculated as the proportion of tested *Ae. aegypti* positive for *w*Mel. Raster cells with no *w*Mel data

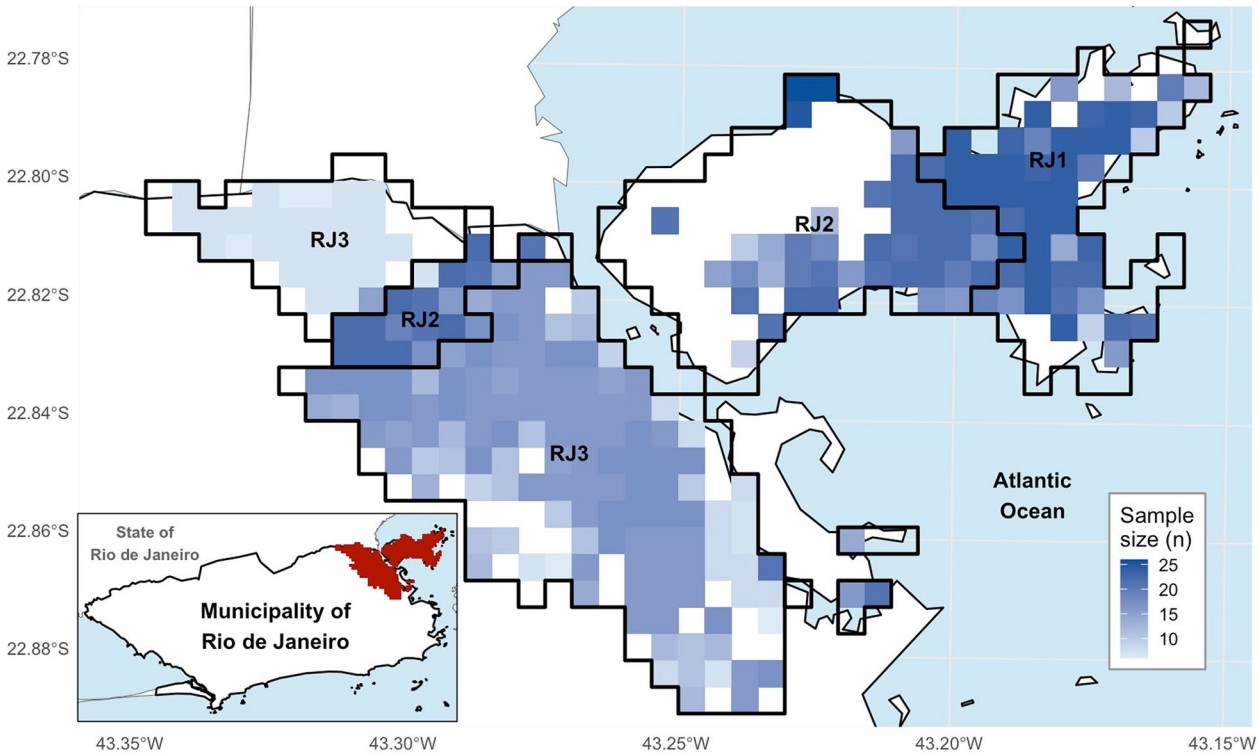


Fig. 1 Map of raster cell sample sizes by *Wolbachia* release zone. Sample size represents the number of months of *Wolbachia* prevalence data available across the total release period. The black outline indicates the total release area ($n=396$). Raster cells with no *w*Mel data ($n=109$) or fewer than 5 months of data ($n=20$) were excluded, leaving 267 raster cells (blue) included in the analysis. The three release zones are labelled RJ1 (releases from August 2017), RJ2 (November 2017), and RJ3 (February 2018, August 2018, and February 2019). The inset shows the municipality of Rio de Janeiro, with the release area highlighted in red

($n=109$) or fewer than 5 months of observations ($n=20$) were excluded, leaving 267 cells (Fig. 1). To standardise heterogeneous follow-up across release areas, a binomial generalised linear model was fitted to each cell and used to generate smoothed 26-month wMel prevalence trajectories from first release. Monthly mean temperature was included to account for irregular sampling and heterogeneous temporal coverage and was not interpreted as an explanatory variable in this step. K-means clustering was then applied to these predicted trajectories to define the categorical outcome used in the environmental regression model. Full details of trajectory derivation are provided in Additional file 1.

Covariates: climate and landscape features

A selection of 23 spatially explicit climate and landscape covariates were compiled, guided by ecological mechanisms influencing the *Ae. aegypti* and *Wolbachia* dynamics. Specifically, covariates focussed on *Ae. aegypti* habitat suitability, climate sensitivity, flight barriers, and *Wolbachia* deployment barriers (Additional file 1: Table S2). Examples from each respective category include human population and vegetation cover, elevation and temperature, proportion of highways and the proportion of non-residential buildings, the proportion of favelas and average household income.

Covariate data were obtained from publicly available sources where possible, harmonised to the 500×500 m grid using area-weighted areal interpolation for partially overlapping polygons and rasters, point-in-polygon summation for point features, and inverse distance-weighted interpolation for climate variables. Covariates related to mosquito dispersal (Additional file 1: Table S2, category: *Ae. aegypti* flight barriers) were extracted within each cell and a surrounding 200 m buffer. Covariates with zero variance were excluded. Highly correlated covariates (coefficients $>|0.8|$) were screened and excluded or transformed as appropriate, driven by ecological interpretability and retaining covariates which are most informative determinants of *Ae. aegypti* distribution. Full details of covariate harmonisation and screening are provided in Additional file 1.

Environmental covariates were included as linear terms rather than smooth functions to maintain model interpretability and avoid overfitting given the relatively small sample size ($n=267$). Preliminary exploration indicated largely monotonic relationships with replacement outcomes, and therefore, non-linear smoothing was applied only to the spatial autocorrelation term. Although covariate effects were modelled linearly on the multinomial logit scale, predicted trajectory probabilities may still exhibit non-linear dynamics due to the multinomial model structure and spatial smooth term.

Model selection

To identify environmental and landscape factors associated with different *w*Mel replacement trajectories, the categorical outcome of cluster assignment was modelled using a GAM in the mgcv R package [60]. Model diagnostics followed standard GAM evaluation procedures including basis dimension diagnostics and residual inspection. GAMs are a common way to model complex and potentially non-linear associations between climate and landscape factors and mosquito ecology [61–65]. Since *Wolbachia* dynamics are mediated through their mosquito hosts, this approach is appropriate for modelling *Wolbachia* replacement and can accommodate spatial autocorrelation.

Forward selection was performed, initially selecting the covariate with greatest reduction in Akaike Information Criterion (AIC) among univariate models and repeating this step to select additional covariates using a stepwise approach until no additional covariates reduce AIC by >2 [66, 67]. Covariate selection was performed prior to including a spatial smooth so that covariates competed without their effects being absorbed by the spatial term [68, 69]. While this approach cannot fully eliminate spatial confounding, it reduces the risk that flexible spatial effects dominate model selection and mask associations with environmental covariates. We considered incorporating spatial terms during model selection as an alternative approach; however, given the limited sample size and spatial resolution, this can lead to unstable estimates when spatial smooths compete with covariates.

Four covariates were selected for inclusion in the model: the proportion of tall buildings (% >6 m in height), average air temperature (°C), average elevation (m above sea level), and average daily rainfall (mm). We modelled the four-level replacement trajectory outcome $\widehat{Y}_c$, defined as the cluster-assigned trajectory category for each raster cell c, using a multinomial GAM. Let $P_{ck} = \Pr(\widehat{Y}_c = k)$ denote the probability that raster cell c belongs to replacement trajectory $k \in \{1, 2, 3, 4\}$, with 1 as baseline. The unsuccessful replacement trajectory was assigned as the reference baseline, since any of the three success trajectories demonstrate some degree of progress towards *Wolbachia* replacement goals. For each of the other trajectories, $k = 2, 3, 4$, the log-odds were modelled as

$$\log\left(\frac{P_{ck}}{P_{c1}}\right) = \alpha_k + \beta_{1k} tall_build_c + \beta_{2k} temp_c + \beta_{3k} elev_c + \beta_{4k} rain_c + f_{k,z(c)}(wMel_c)$$

where $tall_build_c$, $temp_c$, $elev_c$, and $rain_c$ denote, respectively, the proportion of tall buildings (%), average air temperature (°C), average elevation (m above sea level), and average daily rainfall (mm) in raster cell c. α_k is the trajectory-specific intercept, and β_{jk} are the trajectory-specific regression coefficients for each linear covariate j. The multinomial probabilities were obtained using $P_{ck} = \exp(\eta_{ck})/\sum_{m=1}^{4}\exp(\eta_{cm})$, where $\eta_{ck} = \log(P_{ck}/P_{c1})$ for $k = 2, 3, 4$ and $\eta_{c1} = 0$. All covariates were defined at the raster cell level to match the spatial structure of the input data. For each covariate, we derived partial-dependence (PD) curves by trajectory. Local effects were computed as the relative change in predicted probability per trajectory for a specified unit increase in the covariate (finite differences along the PD curve).

Due to strong evidence of spatial autocorrelation, we included a smoothed spatial lag term by release zone to account for local spatial dependence rather than as a predictor of ecological interest (Fig. 1; RJ1, RJ2, RJ3). For each raster cell c, the average proportion of *w*Mel-infected *Ae. aegypti* was estimated in all neighbouring raster cells excluding the focal cell, $wMel_c$, producing a 500–700 m spatial lag (accounting for diagonal cell distance of queen neighbours). Partial dependency plots of the average neighbouring proportion of *w*Mel show the predicted probability of a raster cell being assigned to a replacement trajectory varied across the three release zones. Thus, $f_{k,z(c)}(\bullet)$ is a smooth function of $wMel_c$ estimated using a thin-plate regression spline (bs="ts", $k=10$) for each release zone, z. Smoothness was selected automatically through the mgcv penalisation framework, allowing unnecessary smooth terms to be shrunk towards zero.

Results

The 267 raster cells were first clustered into four replacement trajectory groups: unsuccessful ($n=77$, 28.8%), low ($n=84$, 31.5%), moderate ($n=54$, 20.2%), and high success ($n=52$, 19.5%). Individual raster cell trajectories in any of the low, moderate, or high success groups with a borderline declining slope coefficient (<-0.005) were manually reassigned to the unsuccessful trajectory (moderate success: $n=7$; high success: $n=2$; Additional file 1: Fig. S3). The unsuccessful trajectory was characterised by model-predicted *Wolbachia* prevalence decreasing from 31 to < 20% within 6 months on average, and then declining more slowly reaching a mean of 12% by the end of the release period (Fig. 2). The low- and

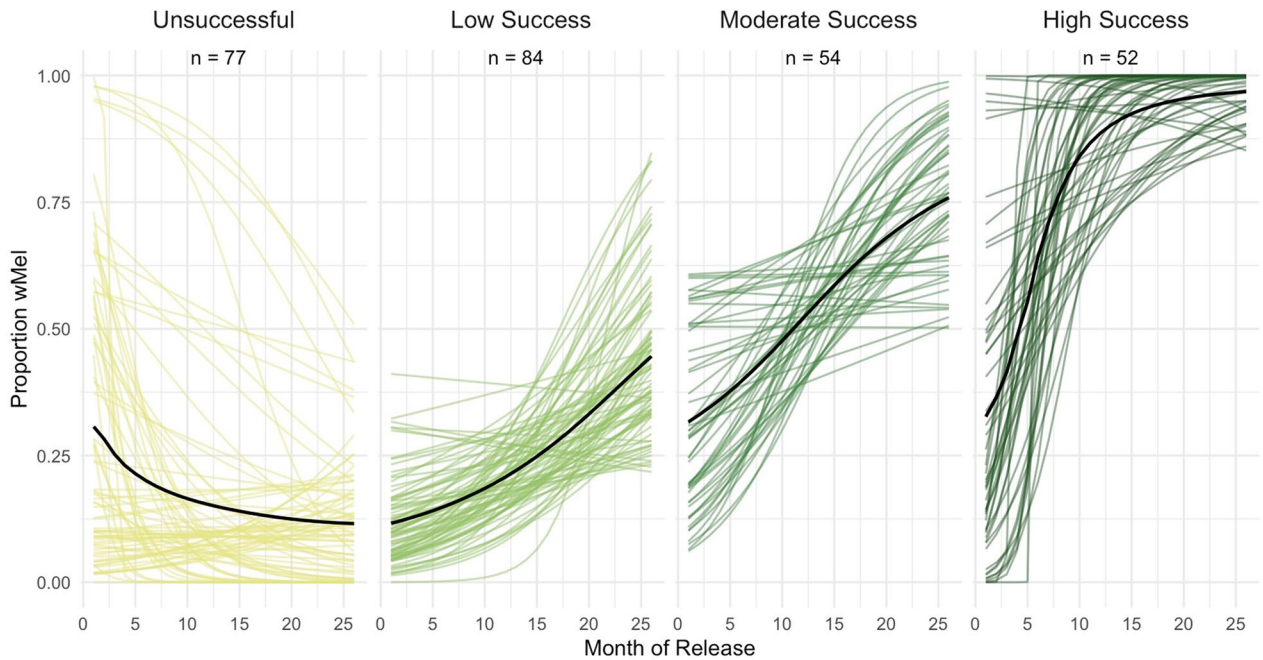


Fig. 2 Model-predicted trajectories of *w*Mel proportion over the release period. Lines show the predicted *w*Mel proportion for each raster cell assigned to each replacement trajectory, with black lines indicating the mean trajectory. Time is expressed as months since the first *Wolbachia* release within each raster cell

moderate-success trajectories increased steadily from 12 to 45% and from 32 to 76% *Wolbachia* prevalence, respectively, whereas the average trend for the high-success trajectory was rapid increase in model-predicted *Wolbachia* prevalence from 33 to > 90% within 13 months on average, eventually stabilising at 96%. Some highly successful raster cells showed little overall change in model-predicted *Wolbachia* prevalence, remaining > 80% throughout the 26-month release period from initial release.

Four covariates were selected for inclusion in the model: the proportion of tall buildings (% > 6 m in height), average air temperature (°C), average elevation (m above sea level), and average daily rainfall (mm). The proportion of tall buildings is a covariate from the category *Ae. aegypti* flight barriers, while the latter three covariates are from the climate sensitivity and breeding habitat covariate categories. To assess the influence of manual trajectory reassignment ($n = 9$), we repeated model selection without trajectory reassignment. The results remained broadly consistent, with the proportion of tall buildings and temperature selected as primary covariates, while some secondary covariates showed minor differences in selection and effect size. Under average environmental and landscape conditions across the release area, the multinomial GAM predicts a baseline probability of 23.9% for unsuccessful replacement, 47.7% for low-success, 22.7% for moderate-success, and 5.7% for high-success trajectories. These were estimated per release zone using zone-specific median covariate values including the spatial lag term, and overall values obtained by weighting zone-level predictions by the number of raster cells. However, there are some notable spatial trends. Monte Carlo Join-Count tests for each group showed strong evidence of spatial autocorrelation (FDR-adjusted $P < 0.01$), showing that replacement trajectories are spatially clustered (Fig. 3) which may also reflect differences in release timing and deployment intensity across zones.

A higher proportion of raster cells show moderate or high success on Ilha do Governador, an island with Rio de Janeiro international airport on the Northwest side (64 of 90, 71.1%), compared to the mainland (42 of 177, 23.7%). Similarly, under median environmental and landscape conditions within release zones, the probability of an area having moderate or high success (61.8% and 12.9%, respectively) is higher for release zone 1 (RJ1), the East side of Ilha do Governador, compared to the other release

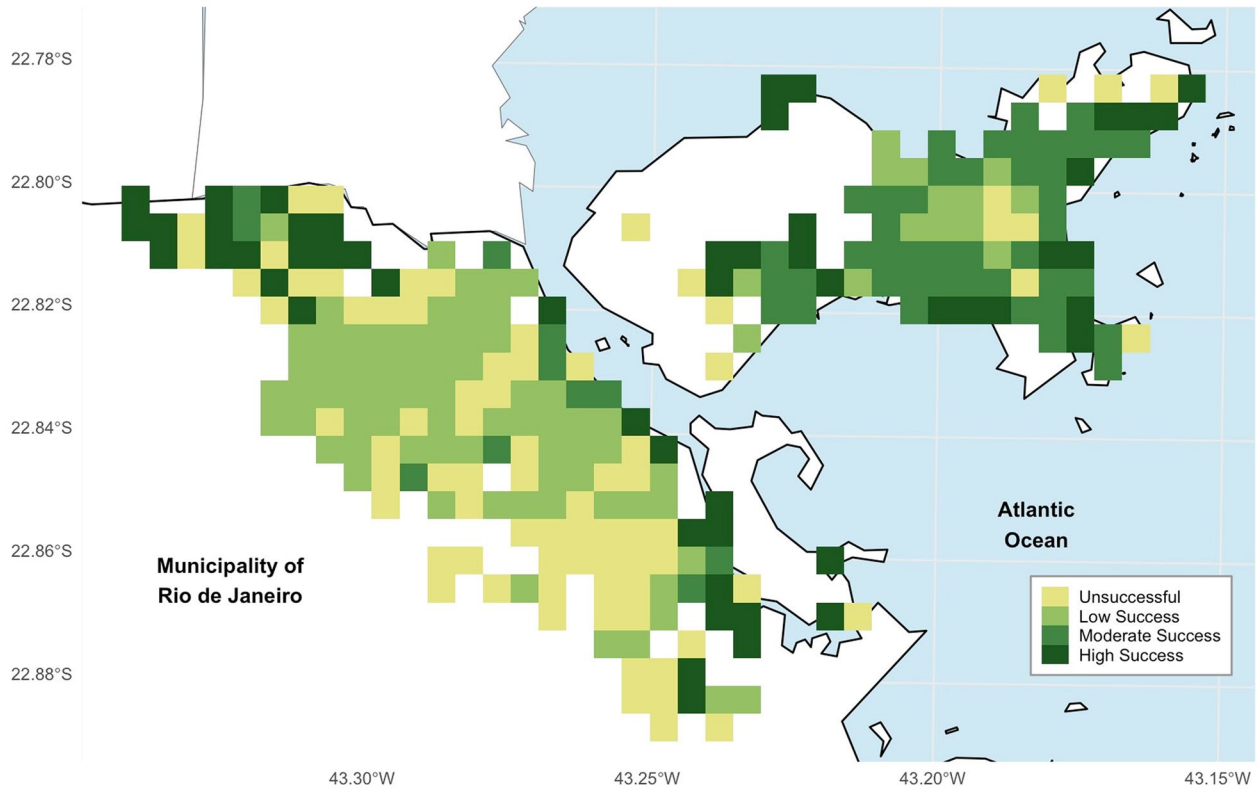


Fig. 3 Spatial distribution of raster cells according to replacement trajectory. Colours indicate the replacement trajectory assigned to each raster cell

Table 1 Median covariate values and baseline model-predicted probability of *Wolbachia* replacement trajectories by release zones (RJ1, RJ2, RJ3)

	RJ1	RJ2	RJ3
Median covariate values			
Proportion of tall buildings (% > 6 m)	0.392	0.400	0.499
Mean air temperature (°C)	24.5	24.5	24.6
Elevation (m)	12.6	12.5	9.11
Mean daily rainfall (mm)	3.58	3.50	3.43
Mean proportion neighbouring *w*Mel (%)	0.347	0.183	0.0894
Baseline model-predicted probability of *Wolbachia* replacement trajectories			
Unsuccessful	10.2%	20.0%	28.5%
Low success	15.1%	40.1%	58.4%
Moderate success	61.8%	35.6%	9.1%
High success	12.9%	4.4%	4.0%

RJ1 is the area on the East side of Ilha do Governador (sample median 23, range 9–24); RJ2 is the area on the West side of Ilha do Governador and expanding onto mainland (sample median 21, range 7–26); RJ3 is the majority of mainland release areas (sample median 15, range 6–21); see Fig. 1 for mapped areas

zones (Table 1). This is consistent with these areas on Ilha do Governador being the first release sites, having more months of releases in total (RJ1 sample median 23, range 9–24, and majority of RJ2 median 21, range 7–26; Fig. 1) before releases expanded West and to the mainland (RJ3 sample median 15, range 6–21). However, inclusion of release zone as a fixed effect in a sensitivity analysis did not improve model fit and did not materially alter the estimated effects of the retained environmental covariates, suggesting that broad differences in release timing and programme duration between zones do not fully explain the observed replacement trajectories. On the mainland, a general trend can be observed where raster cells with moderate or high success tend to be closer to the coastline than inland (Fig. 3) which may be associated with the region's elevation profile, discussed further in the elevation subheading.

Tall buildings

The proportion of tall buildings (% > 6 m in height) was the first covariate selected by the multinomial GAM, ranging from 0.0 to 59.4% (median 47.9%) across the release area (Additional file 1: Fig. S4). High replacement success was strongly associated with a lower proportion of tall buildings [$\beta = -0.93$ (95% CI −1.43, −0.44), $P < 0.001$], whereas low replacement success was strongly associated with a higher proportion of tall buildings [$\beta = 1.10$ (95% CI 0.57, 1.63), $P < 0.001$]. Using model-based predictions, a +10% increase from the median proportion of tall buildings was associated with a 13.5% increase in the probability of low replacement success and reduced probability of all other trajectories (Fig. 4). Sensitivity analyses re-ran model selection sequentially excluding each trajectory, consistently showing that areas with a higher proportion of tall buildings were more likely to experience low replacement success, while areas with fewer tall buildings are more likely to achieve high replacement success.

To investigate the degree of building height associated with *Wolbachia* replacement success, another sensitivity analysis redefined tall buildings as > 15 m in height rather than > 6 m (the next available height category in the dataset; Additional file 1: Table S2). Under this definition, the proportion of tall buildings was no longer strongly collinear with building volume, allowing building volume to be retained during model selection rather than excluded as in the primary analysis. In this sensitivity analysis, building volume was selected first, with the remaining covariates selected in the same order (average air temperature, average elevation, and average daily rainfall). This suggests that when tall buildings are defined at a lower height threshold (> 6 m), the proportion of tall buildings captures much of the same underlying urban structural variation as building volume. While the first selected covariate differs, the findings concur that high urban density and vertical structure (whether measured by height or volume) present a challenge for *Wolbachia* replacement.

Urban structure was also captured by the proportion of vegetation cover, which was the next best performing covariate after rainfall; however, it was not selected as $\Delta AIC < |2|$. When forced in the model, the strength of covariate associations did not noticeably change except within the high success trajectory. In this analysis, high replacement success was significantly associated with a higher proportion of vegetation cover [$\beta = 0.61$ (95% CI 0.09, 1.12), $P = 0.020$], and no longer strongly associated with lower proportions of tall buildings [$\beta = -0.55$ (95% CI −1.15, 0.05), $P = 0.071$]. Suggesting vegetation cover and vertical urban structure may be capturing shared underlying urban characteristics associated with high replacement success trajectory in this sensitivity analysis.

Temperature

Average air temperature (°C) (mean across 26-month release period) was the second covariate selected by the multinomial GAM, ranging from 24.5 to 25.0 °C (median 24.6 °C) (Additional file 1: Fig. S5). High replacement success was strongly associated with higher temperatures within the observed local range [$\beta = 1.11$ (95% CI 0.59, 1.62), $P < 0.001$], a result which was maintained across all sensitivity analyses in which the model was re-run without each trajectory. In the primary analysis, lower temperatures were also strongly associated with moderate

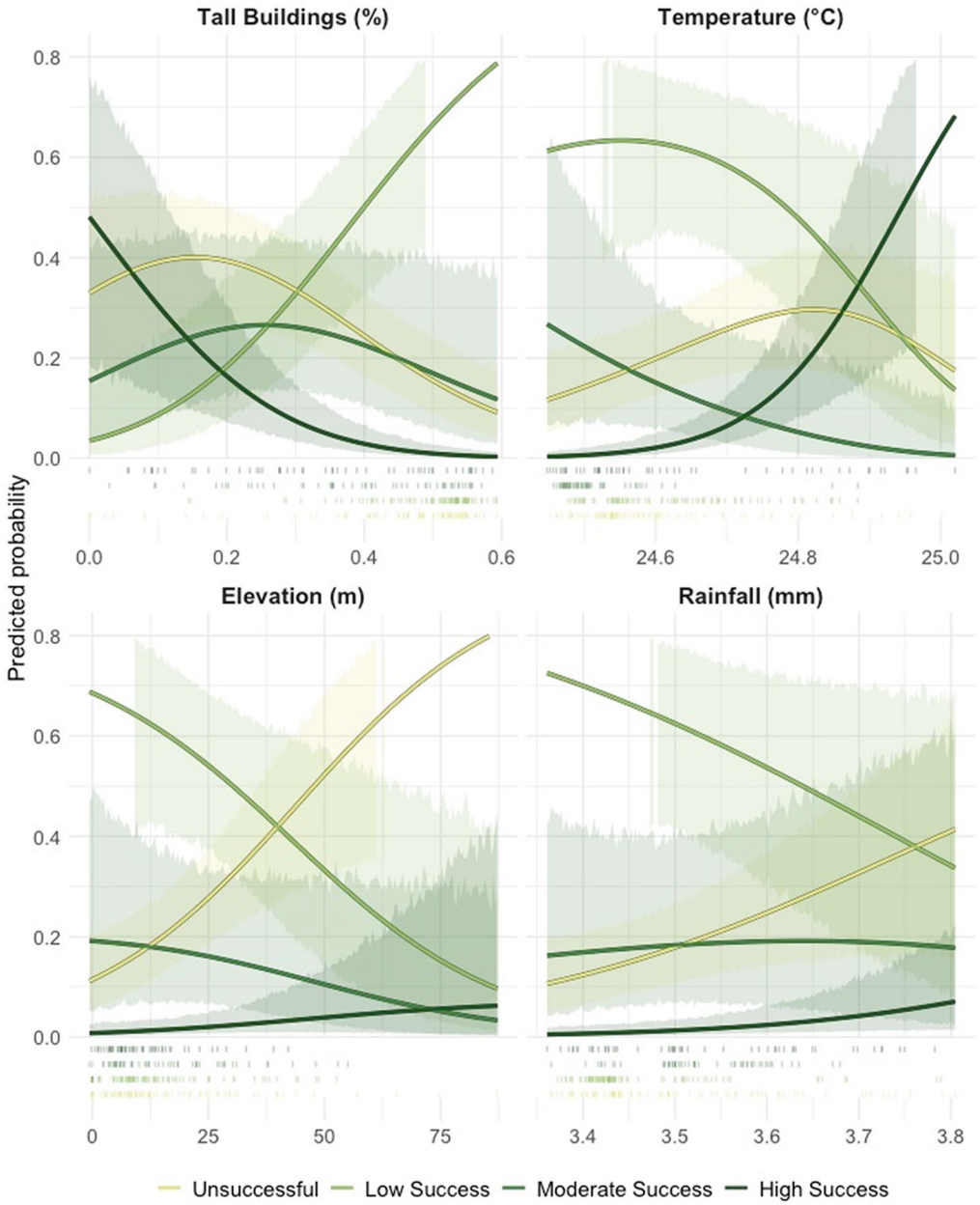


Fig. 4 Partial dependence plots showing the predicted probability of each replacement trajectory across selected model covariates. Panels show the four covariates retained in the final multinomial generalised additive model (GAM): proportion of tall buildings (> 6 m in height), mean air temperature (°C), mean elevation (m), and mean daily rainfall (mm). Coloured lines show the predicted probability of each replacement trajectory. Predictions were generated by varying the focal covariate across its observed range while holding all other continuous covariates, including the spatial smooth term, at their median values and categorical covariates at their reference level. Shaded ribbons represent approximate 95% confidence intervals (CI) derived from the fitted model prediction standard errors. Rug plots beneath each panel indicate the observed distribution of covariate values for each replacement trajectory

replacement success [$\beta = -0.94$ (95% CI −1.81, −0.07), $P < 0.05$], although this result was not maintained through sensitivity analyses.

Using model-based predictions, a + 0.2 °C increase in average air temperature to 24.8 °C is associated with an 11.1% increased probability of *w*Mel replacement failure (unsuccessful). This temperature increase is associated with reduced probability of low replacement

success (−9.5%) and moderate success (−11.2%), yet increased probability of high success (9.6%). Notably, the predictions suggest divergent outcomes, where higher temperatures increase the probability of both high replacement success and replacement failure. The consistency of this bistable trend across temperature and the proportion of tall buildings may be linked to urban heat island effects which have a higher incidence of dengue than other urban areas [70–73].

Elevation

Average elevation (m above sea level) was the third covariate selected by the multinomial GAM. Lower elevation was strongly associated with low ([$\beta = -0.63$ (95% CI −1.04, −0.23), $P < 0.01$] and moderate replacement success [$\beta = -0.59$ (95% CI −1.12, −0.08), $P = 0.024$]. However, elevation ranged from −0.60 to 87.21 m (median 10.86 m) across the release area (Additional file 1: Fig. S5). *Ae. aegypti* are found at high altitude [74, 75], and there is no known biological limitation to *Wolbachia* at elevation; thus, confounding is likely, i.e. the effect of elevation identified by the model captures underlying variation which was not captured in the available covariates or the spatial smooth term. To explore this further, several sensitivity analyses were conducted.

One hypothesis is the higher likelihood of favelas on higher or steeper ground due to the prohibitive cost of building formally organised housing and infrastructure. However, the variable proportion of favelas was not selected by the model. First, we forced the proportion of favelas covariate to be included in the final model which had small positive effect sizes across all trajectories, none significant [$\beta = 0.11$ (95% CI −0.23, 0.45), $\beta = 0.14$ (95% CI −0.30, 0.59), $\beta = 0.10$ (95% CI −0.30, 0.49); low, moderate and high success, respectively]. Elevation effect sizes became marginally smaller, yet overall, no significant changes were observed because of this forced inclusion. Second, we noticed a spatial trend of higher proportion of favelas being clustered either at higher elevation or near the coast, at low elevation. Thus, the proportion of favelas was split by the median elevation into two variables: the proportion of favelas at high and low elevation. Model selection was re-run and there was no change in the covariate selection, i.e. neither favela variable was selected and the elevation variable was still selected. This suggests the proportion of favelas independently and the intersection of favelas at high elevation do not explain this result.

Additionally, changes in urban topology across elevation gradients likely impacted the logistical challenges of deployment. While we do not have access to publicly available data of how many mosquitoes were released in which areas, this could be a key contributor to observed variation in *Wolbachia* replacement trajectories at different elevation. Since elevation may be linked to increased slope gradients, increasing elevation could impact *Ae. aegypti* population dynamics through changes in wind exposure, solar exposure and water runoff, which impacts the effects of rainfall on breeding habitats. Regardless of the underlying mechanism, higher elevation was consistently strongly associated with low replacement success across sensitivity analyses in which the model was re-run without each trajectory. Additionally, model-based predictions suggest that higher elevation is associated with an increased probability of an area having an unsuccessful *w*Mel replacement trajectory (Fig. 4). A +10 m increase in elevation draws *w*Mel replacement trajectories away from low replacement success (−6.4%) and is associated with a 7.3% increased probability of replacement failure (unsuccessful trajectory). Collectively these findings suggest an association between higher elevation and lower likelihood of successful *Wolbachia* replacement in the municipality of Rio de Janeiro, although the underlying mechanisms remain unresolved.

Rainfall

Average daily rainfall (mm) was the fourth and final covariate selected by the multinomial GAM, ranging from 3.36 to 3.80 mm (median 3.48 mm) (Additional file 1: Fig. S5). Lower rainfall was strongly associated with increased risk of low replacement success [$\beta = -0.49$ (95% CI −0.93, −0.06), $P = 0.027$] in the primary analysis. Using model-based predictions, a +0.25 mm increase (median 3.73 mm) shifts *w*Mel replacement trajectories away from low replacement success (probability reduced by 23.3%) while increasing the probability of unsuccessful replacement by 18.9%. The probabilities of moderate and high replacement success change only minimally (+0.6% and 3.9%, respectively), indicating a redistribution from low success towards the extremes, especially replacement failure (Fig. 4). Rainfall is a known ecological driver of *Ae. aegypti* breeding site availability, although its effects are context dependent. However, rainfall was not consistently selected in sensitivity analyses when the model was re-run with individual trajectories excluded, suggesting that its effect on *w*Mel replacement specifically has the weakest support among the four covariates.

Model performance

The multinomial GAM explained 25.3% of the variation in replacement trajectories (percent deviance explained), including the spatial smooth term for neighbouring *w*Mel prevalence. Simpler models including only the spatial smooth term explained substantially less variation (12.8%), indicating that environmental covariates contributed meaningful explanatory power. Model

diagnostics indicated satisfactory model performance as the model converged fully with stable parameter estimation. Basis dimension checks showed no evidence that the spatial smoothing parameter k was insufficient (all k-index ≈0.95, $P > 0.20$) and the estimated degrees of freedom for the spatial smooth ranged from 3×10^{-5} to 1.01 across trajectories, indicating predominantly linear or negligible spatial effects and confirming that the shrinkage spline effectively prevented overfitting [60].

The confusion matrix indicated an overall correct classification rate of trajectory of 0.58 (95% CI 0.52–0.64). Model sensitivity was highest for moderate success and low replacement success (0.70 and 0.65, respectively) and moderate for high success (0.50) and the unsuccessful trajectory (0.47). Specificity exceeded 0.80 for all trajectories, indicating the model was conservative in classification even where sensitivity was limited. However, nearly half of truly unsuccessful cases were misclassified, most frequently as low or high success. This indicates that the model is less reliable for identifying unsuccessful trajectories compared with other trajectories, reflecting trajectory-specific performance differences despite reasonable overall classification accuracy.

Spatial smooth terms for average neighbouring proportion of *w*Mel varied across replacement trajectories. The spatial term was strongly significant for moderate-success trajectories across all release zones (RJ1 $P < 0.01$; RJ2 and RJ3 $P < 0.001$), high-success trajectories across release zones 1 and 2 (RJ1 and RJ2 $P < 0.001$), and low-success trajectories in release zone 3 (RJ3 $P < 0.001$). This indicates the relationship between average neighbouring proportion of *w*Mel and replacement trajectory is dependent on release zone. Analysis of spatial autocorrelation suggested residual spatial structure remained for some trajectories. Moran's I was significant for unsuccessful ($I = 0.070$, $P = 0.034$), low success ($I = 0.145$, $P = 0.001$), and high success ($I = 0.075$, $P = 0.018$), indicating mild spatial clustering of residuals and implying some unexplained spatial structure persists.

Discussion

This study examined how climate and landscape features shape spatially heterogeneous *Wolbachia* replacement in a large-scale urban deployment in the municipality of Rio de Janeiro. By clustering *w*Mel replacement trajectories and modelling their associations with environmental factors, we identified four covariates associated with replacement success: lower proportion of tall buildings (% > 6 m in height), higher air temperature (°C), lower elevation (m above sea level), and higher daily rainfall (mm). Together, these results highlight the importance of urban structure and environmental conditions that influence mosquito dispersal, population connectivity, and life history traits underpinning *Wolbachia* dynamics.

Urban structure, particularly the vertical built environment, emerged as the strongest and most consistent covariate associated with replacement trajectories. Areas with a higher proportion of tall buildings were more likely to exhibit low replacement success, whereas areas with fewer tall buildings were more likely to achieve high success. High-rise clusters can function as semi-permeable barriers to horizontal mosquito dispersal through shading, wind channels, and canyon effects [62, 76, 78 –], and individual buildings represent opportunities for vertical dispersal into distinct habitats [76, 79, 80], potentially reducing effective mixing between released and wild *Ae. aegypti*. One hypothesis is that high-rise buildings create a trade-off in which reduced immigration of uninfected mosquitoes from surrounding areas may facilitate *Wolbachia* invasion by reducing dilution of *Wolbachia* [58], while simultaneously constraining the conditions required for high-level, stable establishment. However, the mechanism remains unknown as tall buildings may also represent urban density, socioeconomic conditions, or release accessibility. Evidence from other *Wolbachia* releases supports how building structure can shape local mosquito dynamics at a fine scale. For example, in Malaysia, *w*AlbB-infected *Ae. aegypti* established across a high-rise residential site with an infection prevalence > 90% within 12 weeks and remained high for at least 5 years [80]. Of the eight residential blocks, some were invaded more rapidly than others and *Wolbachia* frequencies were found to be highest on the 2nd and 8th floors (the middle floor).

Previous metapopulation models predict that *Wolbachia* replacement outcomes depend on local mosquito migration rates and release density [81, 82]. Fine-scale release density data were unavailable for this analysis, and therefore, residual confounding by deployment intensity remains a limitation. Although the data source indicates that releases occurred over extended periods and in multiple phases across the study area [22], adjustment for release zone in a sensitivity analysis produced similar coefficient estimates and did not improve model fit, suggesting that broad differences in release timing and programme duration between zones are unlikely to explain the observed associations. However, release intensity could not be quantified at the spatial resolution of the replacement trajectories analysed here. Consequently, the environmental associations identified should be interpreted as hypothesis-generating and may partially reflect unmeasured variation in deployment intensity or other operational factors. Additionally, host fitness costs linked to insecticide resistance identified in early Rio de Janeiro pilot releases

[59] were addressed operationally prior to the releases analysed here, suggesting that observed heterogeneity is unlikely to be driven solely by host fitness trade-offs, although variation in fitness likely remains.

Sensitivity analyses re-defining tall buildings as > 15 m revealed that building volume became the dominant covariate, indicating that *Wolbachia* success is influenced by broader urban topology rather than building height alone. Vegetation cover, although not selected in the primary analysis, was significantly associated with high replacement success when forced into the model and displaced the importance of tall buildings for this trajectory. This suggests that while tall buildings are the stronger overall covariate distinguishing replacement trajectories, vegetation may reflect habitat suitability factors that could be associated with high-level *Wolbachia* establishment, such as shaded microclimates, resting sites, and stable breeding conditions.

Climate variables further shaped replacement trajectories. Higher temperatures within the observed local range increased the probability of both high replacement success and complete failure while reducing the probability of intermediate trajectories (Fig. 4). This pattern aligns with theoretical expectations that environmental stress can amplify population instability, pushing *Wolbachia* dynamics towards divergent outcomes [83–89], and with threshold-dependent invasion models in which outcomes are governed by unstable internal equilibria and bistability [38, 58, 90]. Mechanistically, these results may reflect a trade-off between the benefits of higher temperatures for *Ae. aegypti*, such as faster development, higher survival and increased fecundity [91–96], and the costs to *Wolbachia,* where cyclical temperature regimes (52,54; 26–37 °C, 23.7–35.3 °C, respectively) or heatwaves [47, 49] can reduce *Wolbachia* infection density or even trigger infection loss [97, 98]. In invasion models, crossing critical thresholds can lead to rapid transitions between persistence and loss of infection. However, this analysis is observational and does not directly identify dynamical attractors or invasion thresholds. The apparent bistability arises from non-linear structure in the fitted multinomial GAM partial-dependence surfaces and should be interpreted as model-based prediction of heterogeneous responses requiring experimental validation.

Elevation was consistently associated with low replacement success and model-predicted probabilities suggested higher elevation is associated with unsuccessful replacement, despite a lack of known biological constraints on *Ae. aegypti* or *Wolbachia* at the elevations observed. This suggests elevation may act as a proxy for unmeasured environmental, infrastructural, socioeconomic, or operational gradients that vary across the urban landscape. A plausible operational explanation may be that favelas present implementation and surveillance challenges which covary with elevation; however, sensitivity analyses exploring the role of hillside favelas did not explain this association. Other factors that may covary with elevation, including differences in vegetation, drainage, road accessibility, housing characteristics, or water storage behaviours, were not directly assessed. Regardless of mechanism, the consistency of this result indicates that elevation-related urban features in the municipality of Rio de Janeiro warrant further investigation to refine release strategies in complex urban landscapes.

Rainfall influenced replacement trajectories by redistributing probability towards low-success trajectories and replacement failure. This broadly aligns with the role of rainfall in generating breeding sites and flushing of immature mosquito stages [39, 40, 99]. However, mechanistic processes were not directly assessed, and rainfall was inconsistently selected across sensitivity analyses, indicating weaker support for its role relative to other covariates.

Mild residual spatial clustering persisted even after incorporating spatial smooth terms, suggesting that neighbourhood-scale processes, including local urban structure, operational deployment intensity and behavioural factors, continue to influence replacement outcomes. Although the overall deviance explained by the model was moderate (25.3%), this is expected in complex urban ecological systems where many operational and behavioural factors remain unmeasured. Classification performance was also moderate, particularly for unsuccessful and high-success trajectories. However, the primary objective of the modelling framework was explanatory rather than predictive, and the identified covariates were associated with gradual shifts in the probability of replacement trajectories. A GAM was selected over alternative machine learning approaches, such as regression trees or random forests, because they provide interpretable estimates of covariate effects while allowing flexible spatial structure [60]. This supports our goal of explanatory inference rather than maximising predictive accuracy. Reliance on publicly available datasets imposed several limitations, for example, aggregation to 500 × 500 m cells, lack of release density data, and reliance on interpolated covariates. In addition, several sociodemographic covariates were derived from the 2022 census, and several environmental covariates were derived from remotely sensed imagery taken between 2019 and 2022, whereas releases occurred between 2017 and 2019. Although many urban landscape characteristics are relatively stable over this timescale, temporal mismatch may have introduced measurement

error for more dynamic variables such as population density, income, and sanitation conditions. Potential limitations also include residual spatial confounding, collinearity among covariates despite screening, and uncertainty associated with the forward AIC model-selection procedure. Although the bootstrap stability analysis demonstrated that the selected covariates were highly consistent across resampled datasets (see Additional file 1), the forward selection procedure evaluated 19 candidate covariates without formal adjustment for multiple testing; thus, the possibility of false-positive covariate selection cannot be excluded. Future studies integrating direct measures of release effort and higher-resolution environmental data could help refine the model and further clarify the drivers of heterogeneous *Wolbachia* replacement.

From an operational perspective, areas with high-rise buildings and topographically complex areas showed more divergent and unpredictable outcomes, sensitive to small perturbations and less likely to stabilise at intermediate replacement. Incorporating urban permeability and vertical structure into predictive models could help identify high-risk areas prior to deployment and inform operational decisions such as increasing release density, modifying release strategies (e.g. targeting individual buildings or floors), or allocating additional monitoring resources. As programmes expand across heterogeneous urban landscapes, replacement data from early deployments can be incorporated into updated models to identify emerging barriers to *Wolbachia* establishment, such as environments where urban structure limits mosquito or *Wolbachia* spread. In this way, modelling and field deployment can operate in a feedback loop in which empirical observations inform model refinement and models in turn guide adaptive adjustments to release strategies and monitoring.

Overall, this study demonstrates that publicly available climate and landscape datasets can generate operationally relevant hypotheses about the drivers of heterogeneous *Wolbachia* replacement. In complex disease systems such as dengue, integrating environmental data with empirical replacement trajectories is a compelling approach for identifying mechanisms underlying spatial variation in intervention outcomes. These findings may inform future field studies and adaptive deployment strategies aimed at improving *Wolbachia* establishment.

Conclusions

Areas characterised by a higher proportion of tall buildings were more prone to divergent *Wolbachia* replacement dynamics in the municipality of Rio de Janeiro, with model-based predictions indicating temperature was associated with increased probabilities of both high success and failure. Incorporating urban permeability and vertical structure into predictive models may help identify areas with greater uncertainty in replacement outcomes prior to deployment and could support operational planning, including considerations such as release density, modifying release strategies (e.g. targeting individual buildings or floors), or prioritising monitoring resources. This work provides a basis for further iterative modelling and field evaluation, where modelling and deployment activities can operate in a feedback loop to better understand barriers to *Wolbachia* establishment.

Supplementary Information

The online version contains supplementary material available at https://doi.org/10.1186/s13071-026-07602-y.

Additional file 1.

Acknowledgements
Not applicable.

Author contributions
KT contributed to conceptualisation, methodology, formal analysis, writing—original draft, writing—review & editing, visualisation, and funding acquisition. KMS contributed to writing—review & editing. SK contributed to provision of resources and writing—review & editing. KMO contributed to conceptualisation, methodology, writing—review & editing, and supervision. OJB contributed to conceptualisation, methodology, writing—review & editing, and supervision. All the authors read and approved the final manuscript.

Funding
This work was supported by the Biotechnology & Biological Sciences Research Council [BB/T008709/1-2546797] assigned to KT. The contents of the published material are solely the responsibility of the individual authors. The funders had no role in study design, data collection and analysis, decision to publish, or preparation of the manuscript.

Data availability
The codebase and associated datasets used in this study are available in the GitHub repository https://github.com/katietiley/wMel_environ_associations_Rio. The *Wolbachia* prevalence dataset analysed during the current study are available in the GitHub repository https://github.com/pdgcam/wMel_Rio_dengue_chik [22].

Declarations

Ethics approval and consent to participate
Not applicable.

Consent for publication
Not applicable.

Competing interests
The authors declare that they have no competing interests.

Author details
[1]Centre for Mathematical Modelling of Infectious Diseases, London School of Hygiene & Tropical Medicine, London, UK. [2]Department of Infectious Disease Epidemiology and Dynamics, Faculty of Epidemiology and Population Health, London School of Hygiene & Tropical Medicine, London, UK. [3]Division of Biosciences, University College London, London, UK. [4]Interdisciplinary Centre for Scientific Computing, Heidelberg University, Heidelberg, Germany. [5]Heidelberg Institute for Geoinformation Technology, Heidelberg, Germany.

Received: 20 March 2026 Accepted: 26 July 2026
Published online: 04 August 2026

nces

1. WHO. Dengue: guidelines for diagnosis, treatment, prevention and control. 2nd ed. Geneva: World Health Organisation; 2009.
2. WHO. Global vector control response 2017–2030. Geneva: World Health Organization; 2017.
3. Kraemer MU, Sinka ME, Duda KA, Mylne AQ, Shearer FM, Barker CM, et al. The global distribution of the arbovirus vectors *Aedes aegypti* and *Ae. albopictus*. Elife. 2015;4:e08347. https://doi.org/10.7554/eLife.08347.012.
4. Ryan SJ, Carlson CJ, Mordecai EA, Johnson LR. Global expansion and redistribution of *Aedes*-borne virus transmission risk with climate change. PLoS Negl Trop Dis. 2018;13:e0007213. https://doi.org/10.1371/journal.pntd.0007213.
5. Ngugi HN, Mutuku FM, Ndenga BA, Musunzaji PS, Mbakaya JO, Aswani P, et al. Characterization and productivity profiles of *Aedes aegypti* (L.) breeding habitats across rural and urban landscapes in western and coastal Kenya. Parasit Vectors. 2017;10:331. https://doi.org/10.1186/s13071-017-2271-9.
6. Simard F, Nchoutpouen E, Toto JC, Fontenille D. Geographic distribution and breeding site preference of *Aedes albopictus* and *Aedes aegypti* (*Diptera*: *Culicidae*) in Cameroon. Central Africa J Med Entomol. 2005;42:726–31.
7. Knerer G, Currie CSM, Brailsford SC. Reducing dengue fever cases at the lowest budget: a constrained optimization approach applied to Thailand. BMC Public Health. 2021;21:807. https://doi.org/10.1186/s12889-021-10747-3.
8. Ndii MZ. Modelling the use of vaccine and *Wolbachia* on dengue transmission dynamics. Trop Med Infect Dis. 2020;5:78. https://doi.org/10.3390/tropicalmed5020078.
9. Biswal S, Reynales H, Saez-Llorens X, Lopez P, Borja-Tabora C, Kosalaraksa P, et al. Efficacy of a tetravalent dengue vaccine in healthy children and adolescents. N Engl J Med. 2019;381:2009–19. https://doi.org/10.1056/nejmoa1903869.
10. Knerer G, Currie CSM, Brailsford SC. The economic impact and cost-effectiveness of combined vector-control and dengue vaccination strategies in Thailand: results from a dynamic transmission model. PLoS Negl Trop Dis. 2020;14:e0008805. https://doi.org/10.1371/journal.pntd.0008805.
11. Mani TR, Arunachalam N, Rajendran R, Satyanarayana K, Dash AP. Efficacy of thermal fog application of deltacide, a synergized mixture of pyrethroids, against *Aedes aegypti*, the vector of dengue. Trop Med Int Health. 2005;10:1298–304. https://doi.org/10.1111/j.1365-3156.2005.01522.x.
12. Hustedt JC, Doum D, Keo V, Ly S, Sam BL, Chan V, et al. Field efficacy of larvivorous fish and pyriproxyfen combined with community engagement on dengue vectors in Cambodia: a randomized controlled trial. Am J Trop Med Hyg. 2021;105:1265–76. https://doi.org/10.4269/ajtmh.20-1088.
13. Andersson N, Nava-Aguilera E, Arosteguí J, Morales-Perez A, Suazo-Laguna H, Legorreta-Soberanis J, et al. Evidence based community mobilization for dengue prevention in Nicaragua and Mexico (Camino Verde, the Green Way): cluster randomized controlled trial. BMJ. 2015;351:h3267. https://doi.org/10.1136/bmj.h3267.
14. Carlson DB, Dale PER, Kurucz N, Dwyer PG, Knight JM, Whelan PI, et al. Mosquito control and coastal development: how they have coexisted and matured in Florida and Australia. J Am Mosq Control Assoc. 2019;35:123–34.
15. Caspari E, Watson GS. On the evolutionary importance of cytoplasmic sterility in mosquitoes. Evolution. 1959;13:568–70.
16. Sinkins SP. *Wolbachia* and cytoplasmic incompatibility in mosquitoes. Insect Biochem Mol Biol. 2004;34:723–9. https://doi.org/10.1016/j.ibmb.2004.03.025.
17. Fine PEM. On the dynamics of symbiote-dependent cytoplasmic incompatibility in Culicine mosquitoes. J Invertebr Pathol. 1978;30:18.
18. Walker T, Johnson PH, Moreira LA, Iturbe-Ormaetxe I, Frentiu FD, McMeniman CJ, et al. The wMel *Wolbachia* strain blocks dengue and invades caged *Aedes aegypti* populations. Nature. 2011;476:450–5. https://doi.org/10.1038/nature10355.
19. Moreira LA, Iturbe-Ormaetxe I, Jeffery JA, Lu G, Pyke AT, Hedges LM, et al. A Wolbachia symbiont in Aedes aegypti limits infection with dengue, chikungunya, and Plasmodium. Cell. 2009;139:1268–78. https://doi.org/10.1016/j.cell.2009.11.042.
20. Gesto JSM, Pinto SB, Dias FBS, Peixoto J, Costa G, Kutcher S, et al. Large-scale deployment and establishment of *Wolbachia* into the *Aedes aegypti* population in Rio de Janeiro, Brazil. Front Microbiol. 2021;12:711107. https://doi.org/10.3389/fmicb.2021.711107.
21. Gesto JSM, Ribeiro GS, Rocha MN, Dias FBS, Peixoto J, Carvalho FD, et al. Reduced competence to arboviruses following the sustainable invasion of *Wolbachia* into native *Aedes aegypti* from Southeastern Brazil. Sci Rep. 2021;11:10039. https://doi.org/10.1038/s41598-021-89409-8.
22. Ribeiro dos Santos G, Durovni B, Saraceni V, Souza Riback TI, Pinto SB, Anders KL, et al. Estimating the effect of the wMel release programme on the incidence of dengue and chikungunya in Rio de Janeiro, Brazil: a spatiotemporal modelling study. Lancet Infect Dis. 2022;22:1587–95. https://doi.org/10.1016/S1473-3099(22)00436-4.
23. Turley AP, Zalucki MP, O'Neill SL, McGraw EA. Transinfected *Wolbachia* have minimal effects on male reproductive success in *Aedes aegypti*. Parasit Vectors. 2013;6:36. https://doi.org/10.1186/1756-3305-6-36.
24. Calle-Tobón A, Rojo-Ospina R, Zuluaga S, Giraldo-Muñoz JF, Cadavid JM. Evaluation of *Wolbachia* infection in *Aedes aegypti* suggests low prevalence and highly heterogeneous distribution in Medellín, Colombia. Acta Trop. 2024;260:107423. https://doi.org/10.1016/j.actatropica.2024.107423.
25. Hien NT, Anh DD, Le NH, Yen NT, Phong TV, Nam VS, et al. Environmental factors influence the local establishment of *Wolbachia* in *Aedes aegypti* mosquitoes in two small communities in central Vietnam. Gates Open Res. 2021;5:147. https://doi.org/10.12688/gatesopenres.13347.1.
26. Pinto SB, Riback TIS, Sylvestre G, Costa G, Peixoto J, Dias FBS, et al. Effectiveness of *Wolbachia*-infected mosquito deployments in reducing the incidence of dengue and other *Aedes*-borne diseases in Niterói, Brazil: a quasi-experimental study. PLoS Negl Trop Dis. 2021;15:e0009556. https://doi.org/10.1371/journal.pntd.0009556.
27. Ogunlade ST, Meehan MT, Adekunle AI, Rojas DP, Adegboye OA, McBryde ES. A review: *Aedes*-borne arboviral infections, controls and *Wolbachia*-based strategies. Vaccines (Basel). 2021;9:1–23. https://doi.org/10.3390/vaccines9010032.
28. Lau MJ, Ross PA, Hoffmann AA. Infertility and fecundity loss of *Wolbachia*-infected *Aedes aegypti* hatched from quiescent eggs is expected to alter invasion dynamics. PLoS Negl Trop Dis. 2021;15:e0009179. https://doi.org/10.1371/journal.pntd.0009179.
29. Ross PA, Hoffmann AA. Fitness costs of *Wolbachia* shift in locally-adapted *Aedes aegypti* mosquitoes. Environ Microbiol. 2022;24:5749–59. https://doi.org/10.1111/1462-2920.16235.
30. Farnesi LC, Belinato TA, Gesto JSM, Martins AJ, Bruno RV, Moreira LA. Embryonic development and egg viability of wMel-infected *Aedes aegypti*. Parasit Vectors. 2019;12:211. https://doi.org/10.1186/s13071-019-3474-z.
31. Allman MJ, Fraser JE, Ritchie SA, Joubert DA, Simmons CP, Flores HA. *Wolbachia*'s deleterious impact on *Aedes aegypti* egg development: the potential role of nutritional parasitism. Insects. 2020;11:1–14. https://doi.org/10.3390/insects11110735.
32. Petersen MT, Couto-Lima D, Garcia GA, Pavan MG, David MR, Maciel-de-Freitas R. Dengue exposure and *Wolbachia* wMel strain affects the fertility of quiescent eggs of *Aedes aegypti*. Viruses. 2023. https://doi.org/10.3390/v15040952.
33. Ross PA, Endersby NM, Yeap HL, Hoffmann AA. Larval competition extends developmental time and decreases adult size of wMelPop *Wolbachia*-infected *Aedes aegypti*. Am J Trop Med Hyg. 2014;91:198–205. https://doi.org/10.4269/ajtmh.13-0576.
34. Turley AP, Moreira LA, O'Neill SL, McGraw EA. *Wolbachia* infection reduces blood-feeding success in the dengue fever mosquito, *Aedes aegypti*. PLoS Negl Trop Dis. 2009. https://doi.org/10.1371/journal.pntd.0000516.
35. Maciel-de-Freitas R, Sauer FG, Kliemke K, Garcia GA, Pavan MG, David MR, et al. *Wolbachia* strains wMel and wAlbB differentially affect *Aedes aegypti* traits related to fecundity. Microbiol Spectr. 2024;12:e00128-24. https://doi.org/10.1128/SPECTRUM.00128-24.

36. Schmidt TL, Filipović I, Hoffmann AA, Rašić G. Fine-scale landscape genomics helps explain the slow spatial spread of *Wolbachia* through the *Aedes aegypti* population in Cairns, Australia. Heredity (Edinb). 2018;120:386–95. https://doi.org/10.1038/s41437-017-0039-9.
37. Regilme MAF, Carvajal TM, Honnen AC, Amalin DM, Watanabeid K. The influence of roads on the fine-scale population genetic structure of the dengue vector *Aedes aegypti* (Linnaeus). PLoS Negl Trop Dis. 2021;15:1–14. https://doi.org/10.1371/journal.pntd.0009139.
38. Turelli M, Barton NH. Deploying dengue-suppressing *Wolbachia*: robust models predict slow but effective spatial spread in *Aedes aegypti*. Theor Popul Biol. 2017;115:45–60. https://doi.org/10.1016/j.tpb.2017.03.003.
39. Tuladhar R, Singh A, Banjara MR, Gautam I, Dhimal M, Varma A, et al. Effect of meteorological factors on the seasonal prevalence of dengue vectors in upland hilly and lowland Terai regions of Nepal. Parasit Vectors. 2019. https://doi.org/10.1186/s13071-019-3304-3.
40. Lega J, Brown HE, Barrera R. *Aedes aegypti* (Diptera: Culicidae) abundance model improved with relative humidity and precipitation-driven egg hatching. J Med Entomol. 2017;54:1375–84. https://doi.org/10.1093/jme/tjx077.
41. Benitez EM, Sangermano F, Ludueña-Almeida FF, Almirón WR, Estallo EL. *Aedes aegypti* in the city of Córdoba: spatial distribution and habitat suitability drivers. J Clim Change Health. 2025;25:100550. https://doi.org/10.1016/j.joclim.2025.100550.
42. Vezzani D, Rubio A, Velázquez SM, Schweigmann N, Wiegand T. Detailed assessment of microhabitat suitability for *Aedes aegypti* (Diptera: Culicidae) in Buenos Aires, Argentina. Acta Trop. 2005;95:123–31. https://doi.org/10.1016/j.actatropica.2005.03.010.
43. Hiscox A, Kaye A, Vongphayloth K, Banks I, Piffer M, Khammanithong P, et al. Risk factors for the presence of *Aedes aegypti* and *Aedes albopictus* in domestic water-holding containers in areas impacted by the Nam Theun 2 hydroelectric project, Laos. Am J Trop Med Hyg. 2013;88:1070–8. https://doi.org/10.4269/ajtmh.12-0623.
44. Godson A, Kumar A. Sewage-driven mosquito proliferation in Urban India: a molecular and environmental correlation study in Coimbatore. Environ Monit Assess. 2025;197:1006. https://doi.org/10.1007/s10661-025-14393-9.
45. Mukhtar MU, Han Q, Liao C, Haq F, Arslan A, Bhatti A. Seasonal distribution and container preference ratio of the dengue fever vector (*Aedes aegypti*, Diptera: Culicidae) in Rawalpindi, Pakistan. J Med Entomol. 2018;55:1011–5. https://doi.org/10.1093/jme/tjy010.
46. Krystosik A, Njoroge G, Odhiambo L, Forsyth JE, Mutuku F, LaBeaud AD. Solid wastes provide breeding sites, burrows, and food for biological disease vectors, and urban zoonotic reservoirs: a call to action for solutions-based research. Front Public Health. 2020;7:405. https://doi.org/10.3389/fpubh.2019.00405.
47. Lopes LES, Ferreira CP, Oliva SM. Exploring the impact of temperature on the efficacy of replacing a wild *Aedes aegypti* population by a *Wolbachia*-carrying one. Appl Math Model. 2023;123:392–405. https://doi.org/10.1016/j.apm.2023.07.007.
48. Hancock PA, Ritchie SA, Koenraadt CJM, Scott TW, Hoffmann AA, Godfray HCJ. Predicting the spatial dynamics of *Wolbachia* infections in *Aedes aegypti* arbovirus vector populations in heterogeneous landscapes. J Appl Ecol. 2019;56:1674–86. https://doi.org/10.1111/1365-2664.13423.
49. Vásquez VN, Kueppers LM, Rašić G, Marshall JM. wMel replacement of dengue-competent mosquitoes is robust to near-term change. Nat Clim Chang. 2023;13:848–55. https://doi.org/10.1038/s41558-023-01746-w.
50. Ross PA, Ritchie SA, Axford JK, Hoffmann AA. Loss of cytoplasmic incompatibility in *Wolbachia*-infected *Aedes aegypti* under field conditions. PLoS Negl Trop Dis. 2019;13:e0007357. https://doi.org/10.1371/journal.pntd.0007357.
51. Ulrich JN, Beier JC, Devine GJ, Hugo LE. Heat sensitivity of wMel *Wolbachia* during *Aedes aegypti* development. PLoS Negl Trop Dis. 2016;10:e0004873. https://doi.org/10.1371/journal.pntd.0004873.
52. Ross PA, Wiwatanaratanabutr I, Axford JK, White VL, Endersby-Harshman NM, Hoffmann AA. *Wolbachia* infections in *Aedes aegypti* differ markedly in their response to cyclical heat stress. PLoS Pathog. 2017;13:e1006006. https://doi.org/10.1371/journal.ppat.1006006.
53. Velez ID, Uribe A, Barajas J, Uribe S, Ángel S, Suaza-Vasco JD, et al. Large-scale releases and establishment of wMel *Wolbachia* in *Aedes aegypti* mosquitoes throughout the cities of Bello, Medellín and Itagüí, Colombia. PLoS Negl Trop Dis. 2023;17:e0011642. https://doi.org/10.1371/journal.pntd.0011642.
54. Zheng B, Tang M, Yu J, Qiu J. *Wolbachia* spreading dynamics in mosquitoes with imperfect maternal transmission. J Math Biol. 2018;76:235–63. https://doi.org/10.1007/s00285-017-1142-5.
55. Campo-Duarte DE, Vasilieva O, Cardona-Salgado D, Svinin M. Optimal control approach for establishing wMelPop *Wolbachia* infection among wild *Aedes aegypti* populations. J Math Biol. 2018;76:1907–50. https://doi.org/10.1007/s00285-018-1213-2.
56. Reyna-Lara A, Soriano-Paños D, Arias-Castro JH, Martínez HJ, Gómez-Gardeñes J. A metapopulation approach to identify targets for *Wolbachia*-based dengue control. Chaos. 2022;32:041105. https://doi.org/10.1063/5.0087435.
57. Hancock PA, White VL, Ritchie SA, Hoffmann AA, Godfray HCJ. Predicting *Wolbachia* invasion dynamics in *Aedes aegypti* populations using models of density-dependent demographic traits. BMC Biol. 2016;14:96. https://doi.org/10.1186/s12915-016-0319-5.
58. Hancock PA, Godfray HCJ. Modelling the spread of *Wolbachia* in spatially heterogeneous environments. J R Soc Interface. 2012;9:3045–54. https://doi.org/10.1098/rsif.2012.0253.
59. Garcia G, Sylvestre G, Aguiar R, da Costa GB, Martins AJ, Lima JBP, et al. Matching the genetics of released and local *Aedes aegypti* populations is critical to assure *Wolbachia* invasion. PLoS Negl Trop Dis. 2019. https://doi.org/10.1371/journal.pntd.0007023.
60. Wood SN. Generalized additive models: an introduction with R. 2nd ed. New York: Chapman and Hall/CRC; 2017. https://doi.org/10.1201/9781315370279.
61. Sehi GT, Birhanie SK, Hans J, Brown MQ, Parker DM. Environmental correlates of *Aedes aegypti* abundance in the West Valley region of San Bernardino County, California, USA, from 2017 to 2023: an ecological modeling study. Parasit Vectors. 2025;18:349. https://doi.org/10.1186/s13071-025-06967-w.
62. Tewari P, Guo P, Dickens B, Ma P, Bansal S, Lim JT. Associations between dengue incidence, ecological factors, and anthropogenic factors in Singapore. Viruses. 2023;15:1917. https://doi.org/10.3390/v15091917.
63. Cavany SM, España G, Lloyd AL, Vazquez-Prokopec GM, Astete H, Waller LA, et al. Fusing an agent-based model of mosquito population dynamics with a statistical reconstruction of spatio-temporal abundance patterns. PLoS Comput Biol. 2023;19:e1010424. https://doi.org/10.1371/journal.pcbi.1010424.
64. Chaves LF, Morrison AC, Kitron UD, Scott TW. Nonlinear impacts of climatic variability on the density-dependent regulation of an insect vector of disease. Glob Chang Biol. 2012;18:457–68. https://doi.org/10.1111/j.1365-2486.2011.02522.x.
65. Ludwig A, Rousseu F, Kotchi SO, Allostry J, Fournier RA. Mapping the abundance of endemic mosquito-borne diseases vectors in Southern Quebec. BMC Public Health. 2023;23:924. https://doi.org/10.1186/s12889-023-15773-x.
66. Akaike H. A new look at the statistical model identification. IEEE Trans Automat Contr. 1974;19:716–23. https://doi.org/10.1109/TAC.1974.1100705.
67. Burnham KP, Anderson DR. Model selection and multimodel inference: a practical information-theoretic approach. 2nd ed. New York: Springer-Verlag; 2002. https://doi.org/10.1007/b97636.
68. Dupont E, Wood SN, Augustin NH. Spatial+: a novel approach to spatial confounding. Biometrics. 2022;78:1279–90. https://doi.org/10.1111/biom.13656.
69. Hodges JS, Reich BJ. Adding spatially-correlated errors can mess up the fixed effect you love. Am Stat. 2010;64:325–34. https://doi.org/10.1198/tast.2010.10052.
70. de Azevedo TS, Bourke BP, Piovezan R, Sallum MAM. The influence of urban heat islands and socioeconomic factors on the spatial distribution of *Aedes aegypti* larval habitats. Geospat Health. 2018;13:179–87. https://doi.org/10.4081/gh.2018.623.
71. Sureshkumar S, Shekhar S. Impact of urban heat island effect on dengue incidence: A remotesensing approach using thermal and high-resolution optical imagery. BMC Public Health 2025;25;2914https://doi.org/10.1186/s12889-025-23763-4.
72. Araujo RV, Albertini MR, Costa-da-Silva AL, Suesdek L, Franceschi NCS, Bastos NM, et al. São Paulo urban heat islands have a higher incidence of

dengue than other urban areas. Braz J Infect Dis. 2015;19:146–55. https://doi.org/10.1016/j.bjid.2014.10.004.
73. Santos JPC, Honório NA, Barcellos C, Nobre AA. A perspective on inhabited urban space: land use and occupation, heat islands, and precarious urbanization as determinants of territorial receptivity to dengue in the city of Rio de Janeiro. Int J Environ Res Public Health. 2020;17:1–20. https://doi.org/10.3390/ijerph17186537.
74. Dhimal M, Gautam I, Joshi HD, O'Hara RB, Ahrens B, Kuch U. Risk factors for the presence ofchikungunya and dengue vectors (Aedes aegyptiandAedes albopictus), their altitudinaldistribution and climatic determinants of their abundance in Central Nepal. PLoS Negl Trop Dis 2015;9;e0003545.https://doi.org/10.1371/journal.pntd.0003545.
75. Lozano-Fuentes S, Hayden MH, Welsh-Rodriguez C, Ochoa-Martinez C, Tapia-Santos B, Kobylinski KC, et al. The dengue virus mosquito vector *Aedes aegypti* at high elevation in México. Am J Trop Med Hyg. 2012;87:902–9. https://doi.org/10.4269/ajtmh.2012.12-0244.
76. Lau KW, Chen CD, Lee HL, Asri-Isa M, Zulfadli M, Sofian-Azirun M. Vertical distribution of *Aedes* mosquitoes in multiple storey buildings in Selangor and Kuala Lumpur. Malaysia Trop Biomed. 2013;30:36–45.
77. Jayathilake TA, Hasini DG, Wickramasinghe MB, de Silva BGD, Nissanka K. Oviposition and vertical dispersal of *Aedes* mosquitoes in multiple storey buildings in Colombo district. Sri Lanka J Vector Borne Dis. 2015;52:245–51.
78. Liao JR, Tu WC, Chiu MC, Kuo MH, Cheng HC, Chan CC, et al. Joint influence of architectural and spatiotemporal factors on the presence of *Aedes aegypti* in urban environments. Pest Manag Sci. 2023;79:4367–75. https://doi.org/10.1002/ps.7634.
79. Hamid NA, Mohd Noor SN, Isa NR, Md Rodzay R, Effendi AMB, Hafisool AA, et al. Vertical infestation profile of *Aedes* in selected urban high-rise residences in Malaysia. Trop Med Infect Dis. 2020;5:114. https://doi.org/10.3390/tropicalmed5030114.
80. Cheong YL, Nazni WA, Lee HL, NoorAfizah A, MohdKhairuddin IC, Kamarul GMR, et al. Spatial distribution and long-term persistence of *Wolbachia*-infected *Aedes aegypti* in the Mentari Court, Malaysia. Insects. 2023;14:373. https://doi.org/10.3390/insects14040373.
81. Guevara-Souza M, Vallejo EE. A computer simulation model of *Wolbachia* invasion for disease vector population modification. BMC Bioinformatics. 2015;16:317. https://doi.org/10.1186/s12859-015-0746-2.
82. Dye D, Cain JW. Efficacy of *Wolbachia*-based mosquito control: predictions of a spatially discrete mathematical model. PLoS ONE. 2024;19:e0297964. https://doi.org/10.1371/journal.pone.0297964.
83. Sallet G, Silva Moacyr AHB. Monotone dynamical systems and some models of *Wolbachia* in *Aedes aegypti* populations. Rev Afr Rech Inform Math Appl. 2015;20:145–76. https://doi.org/10.46298/arima.1992.
84. Koiller J, da Silva M, Souza M, Codeço C, Iggidr A, Sallet G et al. *Aedes*, *Wolbachia* and Dengue. Villers-Lès-Nancy, France; 2014.
85. Zhang X, Tang S, Cheke RA. Models to assess how best to replace Dengue virus vectors with *Wolbachia*-infected mosquito populations. Math Biosci. 2015;269:164–77. https://doi.org/10.1016/j.mbs.2015.09.004.
86. Zheng B, Guo W, Hu L, Huang M, Yu J. Complex *Wolbachia* infection dynamics in mosquitoes with imperfect maternal transmission. Math Biosci Eng. 2018;15:523–41. https://doi.org/10.3934/mbe.2018024.
87. Qu Z, Xue L, Hyman JM. Modeling the transmission of *Wolbachia* in mosquitoes for controlling mosquito-borne diseases. SIAM J Appl Math. 2018;78:826–52. https://doi.org/10.1137/17M1130800.
88. Xue L, Manore CA, Thongsripong P, Hyman JM. Two-sex mosquito model for the persistence of *Wolbachia*. J Biol Dyn. 2017;11:216–37. https://doi.org/10.1080/17513758.2016.1229051.
89. Vicencio D, Vasilieva O, Gajardo P. Monotonicity properties arising in a simple model of *Wolbachia* invasion for wild mosquito populations. Math Biosci Eng. 2023;20:1148–75. https://doi.org/10.3934/mbe.2023053.
90. Hancock PA, Sinkins SP, Godfray HCJ. Population dynamic models of the spread of *Wolbachia*. Am Nat. 2011;177:323–33. https://doi.org/10.1086/658121.
91. Kamimura K, Matsuse IT, Takahashi H, Komukai J, Fukuda T, Suzuki K, et al. Effect of temperature on the development of *Aedes aegypti* and *Aedes albopictus*. Med Entomol Zool. 2002;53:53–8.
92. Beserra EB, Fernandes CRM, De SA, Silva O, Da Silva LA, Dos Santos JW. Effects of temperature on life cycle, thermal exigency and number of generations per year estimation of *Aedes aegypti* (Diptera, Culicidae). Iheringia Ser Zool. 2009;99:142–8.
93. Rueda LM, Patel KJ, Axtell RC, Stinner RE. Temperature-dependent development and survival rates of *Culex quinquefasciatus* and *Aedes aegypti* (Diptera: Culicidae). J Med Entomol. 1990;27:892–8.
94. Focks DA, Haile DG, Daniels E, Mount GA. Dynamic life table model for *Aedes aegypti* (Diptera: Culicidae): analysis of the literature and model development. J Med Entomol. 1993;30:1003–17.
95. Tun-Lin W, Burkot TR, Kay BH. Effects of temperature and larval diet on development rates and survival of the dengue vector *Aedes aegypti* in north Queensland, Australia. Med Vet Entomol. 2000;14:31–7. https://doi.org/10.1046/j.1365-2915.2000.00207.x.
96. Yang HM, Macoris MLG, Galvani KC, Andrighetti MTM, Wanderley DMV. Assessing the effects of temperature on the population of *Aedes aegypti*, the vector of dengue. Epidemiol Infect. 2009;137:1188–202. https://doi.org/10.1017/S0950268809002040.
97. Mancini MV, Ant TH, Herd CS, Martinez J, Murdochy SM, Gingell DD, et al. High temperature cycles result in maternal transmission and dengue infection differences between *Wolbachia* strains in *Aedes aegypti*. MBio. 2021;12:e00250-21.
98. Hague MTJ, Wheeler TB, Cooper BS. Comparative analysis of *Wolbachia* maternal transmission and localization in host ovaries. Commun Biol. 2024;7:727. https://doi.org/10.1038/s42003-024-06431-y.
99. Montgomery MJ, Harwood JF, Yougang AP, Wilson-Bahun TA, Tedjou AN, Keumeni CR, et al. The effects of urbanization, temperature, and rainfall on *Aedes aegypti* and *Aedes albopictus* mosquito abundance across a broad latitudinal gradient in Central Africa. Parasit Vectors. 2025;18:135. https://doi.org/10.1186/s13071-025-06764-5.

Publisher's Note

Springer Nature remains neutral with regard to jurisdictional claims in published maps and institutional affiliations.